

## Original Article

## Embolic Effects of *Bletilla striata* Microspheres in Renal Artery and Transplanted VX2 Liver Tumor Model in Rabbits\*

LUO Shi-hua<sup>1</sup>, SONG Song-lin<sup>1</sup>, ZHENG Chuan-sheng<sup>1</sup>, LI Wei-yong<sup>2</sup>,  
WANG Yong<sup>1</sup>, XIA Xiang-wen<sup>1</sup>, and FENG Gan-sheng<sup>1</sup>

**ABSTRACT** **Objective:** To evaluate the characteristics of *Bletilla striata* microspheres (BSMs) and its effects as an embolic agent in a rabbit model. **Methods:** BSMs were prepared with an emulsification-cool condensation-chemical cross-linking method. The characteristics of BSMs *in vitro* were observed. Embolization experiments were performed in renal artery of rabbit and in a rabbit liver VX2 carcinoma model. Seventy-two New Zealand rabbits were divided into 2 groups, and the right renal artery was embolized with BSMs (200  $\mu$ m in diameter) in the experimental group and with polyvinyl alcohol (PVA) of the same size in the control group. The pathological findings were examined with hematoxylin-eosin and Masson stainings. Liver and renal functions were tested before and after embolization. VX2 tumor was transplanted in 15 New Zealand rabbits, which were randomly divided into 3 groups ( $n=5$ ). Group A were treated with saline, group B with a mixture of doxorubicin and lipiodol, and group C with hepatic arterial infusion of BSMs (200  $\mu$ m in diameter). Tumor growth rate was evaluated by magnetic resonance imaging scan. Apoptosis-related factors (bax, bcl-2) and tumor vascular endothelial cell growth factor (VEGF) were evaluated through immunohistochemical staining. **Results:** The characteristics of BSMs *in vitro* were in full compliance with the requirements for use in interventional procedures. In the renal artery embolization experiment, after BSMs intervention, it was more difficult to form collateral circulation than that with PVAs, and the kidney manifested atrophy and calcification. There were no significant difference of liver and renal functions in rabbits between groups. In the liver VX2 carcinoma embolization experiment, compared with group A, the growth rate of VX2 liver tumor and Bcl-2 levels was reduced, while apoptosis index, Bax, and VEGF were increased in group B ( $P<0.05$ ). There were no significant difference between groups B and C ( $P>0.05$ ). **Conclusions:** The characteristics of BSMs *in vitro* and *in vivo* meet the requirements for its use as an embolic agent in interventional approaches.

**KEYWORDS** *Bletilla striata*, Chinese medicine, microsphere, characteristic, embolization

Transcatheter-arterial embolization (TAE) has been widely accepted for its efficacy and is used to treat various diseases, including tumors, vascular lesions, and hemorrhages. Various embolic materials have been developed and utilized. A variety of microspheres have been developed as embolic agents. Intra-arterial embolization with microspheres are applied to the level of arteriole by means of endovascular catheters on the basis of particle size.<sup>(1)</sup> The major advantage of microspheres lies in their potential to be injected through small flow-directed and ease of manipulation. For a given particle and vessel size, microspheres penetrate to a much greater extent than other embolic agents and are well-distributed in target vessels with powerful embolization in the peripheral vessels, fewer collateral circulation formation and non-selectivity.<sup>(2,3)</sup>

Our group has conducted a series of studies

on the Chinese herb, *Bletilla striata*, since the last century, and has confirmed that the *Bletilla striata* polysaccharide is an embolic agent that has a powerful embolic effect. Specifically, it is an extraordinary carrier and can inhibit angiogenesis and collateral circulation after TAE.<sup>(4-6)</sup> Mucopolysaccharide is the main component of *Bletilla*

©The Chinese Journal of Integrated Traditional and Western Medicine Press and Springer-Verlag Berlin Heidelberg 2017

\*Supported by the Department of Pharmacy, Union Hospital, Tongji Medical College, Huazhong University of Science and Technology

1. Department of Radiology, Union Hospital, Tongji Medical College, Huazhong University of Science and Technology, Wuhan (430022), China; 2. Department of Pharmacy, Union Hospital, Tongji Medical College, Huazhong University of Science and Technology, Wuhan (430022), China

Correspondence to: Prof. ZHENG Chuan-sheng, Tel: 86-27-85726432, E-mail: [hqzcsxh@sina.com](mailto:hqzcsxh@sina.com)

DOI: <https://doi.org/10.1007/s11655-017-2953-3>

*striata*, which consists of four mannose molecules and one glucose molecule that isopolymerized.<sup>(7)</sup> *Bletilla striata* polysaccharide is slightly soluble in aqueous solutions, forming a hydrophilic *Bletilla striata* gel, and is insoluble in organic solvents. Without antigenicity and toxic side effects in tissues, it has been widely used in Eastern Asian countries to treat alimentary canal mucosal damage, ulcer, bleeding, bruises, burns and tumors.<sup>(8,9)</sup> This study is an extension of our series of research on *Bletilla striata*. We extracted *Bletilla striata* polysaccharide with a modified method and prepared blank *Bletilla striata* microspheres (BSMs). This study aimed to determine the basic characteristics of these new BSMs, including their embolic behavior when used as embolic materials in the rabbit renal arteries and the VX2 liver tumor model.

## METHODS

### Preparation of BSMs

*Bletilla striata* polysaccharide was prepared by ethanol precipitation, followed by 60 °C water extraction, deproteinization with the Sevag method,<sup>(7)</sup> petroleum ether (Sinopharm Chemical Reagent Co., China) defatting and activated carbon (Sinopharm Chemical Reagent Co.) bleaching. It was further isolated by ion-exchange chromatography on a DE-52 column (Whatman Co., America) and gel filtration on a Sephadex G-100 column (Whatman Co., America), yielding purified *Bletilla striata* polysaccharide. BSMs were prepared according to the modified method of emulsion-condensation-chemical cross linking. The microspheres were sized by passing them through sieves with different apertures. They were then placed into bottles based on sphere size, packaged and sterilized.

### Characteristic Test of BSMs *In Vitro*

The surface morphology of the BSMs was observed using an environmental scanning electron microscope (FEI Co., Eindhoven, Netherland). The diameter of the microspheres was measured with a laser particle size analyzer (Malvern Instruments Ltd., Worcestershire, UK). Different concentrations (20%, 30% and 50%) of microspheres were prepared in Omnipaque (Omnipaque 350; GE Healthcare, China) in flasks, oscillated for 2 min and allowed to stand. The microsphere dispersion, suspension and settling time were observed. The settling time for microspheres was measured from the start until they had completely settled on the bottom of flask. Then,

predefined amounts of microspheres were added to normal saline, omnipaque, sodium acetate buffer (pH 6.45, 7.00 and 8.45) in 5 tubes (0.8 cm × 10 cm). After oscillating for 1 min and standing, the diameter of the microspheres were measured before swelling with a light microscope (Shimadzu Corporation, Tokyo, Japan). Then, 10 mg of different sized BSMs (50–100, 100–200, 200–300, 300–400, 400–500, and 500–700 μm in diameter) were added to 10 mL of saline and omnipaque in the preparation of the suspensions. The suspension was injected into a 5Fand2.7F SP micro-catheter (Terumo Corporation, Japan) with a 2-mL syringe to observe the shape of microspheres. The catheter was rinsed with normal saline before each test. In addition, 10 mg BSMs of 200–300 and 500–700 μm in diameter were added into a small flask filled with saline at 37 °C. At different observation time points, the analysis of BSMs degradation was performed by measuring the change in shape of the particle.

### Embolization Experiment of BSMs in Rabbit Models

The study protocol was approved by the Animal Experimentation Committee and the experiments were performed according to the Animal Care Guidelines of Tongji Medical College. New Zealand rabbits (whether male or female, weighing 2.0–2.5 kg) were purchased from Laboratory Animal Center of Tongji Medical College, Huazhong University of Science and Technology, with certification No. SCXK (E) 2011-0011. Animals were kept in the environment of 20 °C, 45%–65% humidity and reasonable lighting, with nutrient diet and high pressure sterilization water.

### Embolization of Renal Artery

The BSMs (200 μm) were sterilized with <sup>60</sup>Co-γ irradiation for animal experiments. PVAs of the same size (COOK Co., America) were used as controls. A total of 72 New Zealand rabbits were randomly divided according to laboratory animal number into an experiment group ( $n=36$ , embolized with BSMs) and a control group ( $n=36$ , embolized with PVAs), and 9 observation time points after embolization were set (1, 3, 7 days, 2, 3, 4, 6, 8 and 12 weeks,  $n=4$  each). Before embolization, baseline liver and renal functions were tested. In the process of renal embolization, general anesthesia was administered intramuscularly to each rabbit. The right femoral artery was surgically exposed, and a 4-Fr sheath (Terumo Corporation,

Tokyo, Japan) was inserted with a cut-down method under fluoroscopy. The trunk of the renal artery was selected using a 4-Fr cobra-type catheter (Terumo Corporation), and renal arteriography was performed by manual injection of 2 mL omnipaque, diluted by 50%. The renal artery was embolized immediately after the administration of a mixture of BSMs. At each time point after embolization, angiography and pathologic examination of kidneys, as well as liver and renal function tests (enzyme coupling spectrophotometry, ROCHE), were performed to detect aspartic transaminase (AST), alanine aminotransferase (ALT), creatine (Cre) and blood urea nitrogen (BUN) levels. Renal angiography was used to evaluate the duration of embolization and collateral circulation formation, with the contralateral kidney as a comparison. The gross pathology of the kidneys, including color, size and weight were also observed. Paraffin-embedded kidney tissue sections were stained with hematoxylin-eosin (HE) and Masson stainings. Vascular fibers were observed after embolization induced renal tissue necrosis. The distribution of embolic agents, as well as the target vessel recanalization and inflammation, were observed. Lung tissue was also observed by HE staining.

### Embolization Experiment in Rabbit Liver VX2 Carcinoma Model

VX2 tumor was transplanted in the left liver lobes of 15 New Zealand rabbits. According to laboratory animal number, the rabbits were randomly divided into 3 groups of 5 animals each by random number table as follows: group A underwent hepatic arterial infusion of saline, group B received hepatic arterial infusion of a mixture of lipiodol (lipiodol ultra-fluid; Guerbet, France) and doxorubicin, and group C received BSMs. All animals received magnetic resonance imaging (Magnetom Avanto; Siemens Medical Solutions, Germany) scanning of the abdomen before and 2 weeks after interventional therapy. Tumor volume ( $V_{pre}$ ,  $V_{post}$ ) was calculated by the formula  $V=0.5 \times a \times b^2$  ( $a$ : maximum longitudinal diameter,  $b$ : maximum transverse diameter) and tumor growth rate (GR,  $GR=[V_{post}-V_{pre}]/V_{pre} \times 100\%$ ) was also calculated. After 2 weeks of therapy, DSA (Angiostar Plus, Siemens Medical Solutions) was performed again to evaluate the status of recanalization and collateral circulation formation.

The animals were euthanized to harvest

specimens, including the tumor and adjacent normal liver tissue. Pathological examination was performed to observe the morphology and the distribution of embolic agents. Immunohistochemical staining was further performed to evaluate apoptosis-related factors (bax, bcl-2; Boster Co., China) and tumor vascular endothelial cell growth factor (VEGF; Boster Co.). The apoptosis of tumor cells was also evaluated by the terminal deoxynucleotidyl transferase UTP nick end labeling (TUNEL) method, the positive cells in each of 100 cells were regarded as apoptosis index (AI). All slides were reviewed with HMIAS-2000 analysis system (Champion Image Co., China) and percentage of positive expression was scored by two independent observers in blind. A few cases with discrepant scores were reevaluated to reach a final agreement.

For the interventional procedure, the right common femoral artery cut down was performed surgically. A 4-F sheath was then slowly inserted, followed by a 4-F catheter with a tip in the shape of a hockey stick, which was first advanced into the aorta and then into the celiac trunk and common hepatic artery. Arteriography of the common hepatic artery demonstrated the hepatic arterial anatomy and the location, size and vascularity of the tumor. Then, the 2.7F catheter was advanced over the 0.014-inch guide wire and into the left hepatic artery, following which the mixture of drugs was infused into the artery.

### Statistical Analysis

Data analysis was carried out by GraphPad Prism 5 software (GraphPad, San Diego, US). Quantitative data were expressed as mean  $\pm$  standard deviation ( $\bar{x} \pm s$ ). Significance between groups was established using the  $\chi^2$  tests. A  $P$ -value less than 0.05 was considered statistically significant.

## RESULTS

### Characteristic Test of BSMs *In Vitro*

Scan-electron microscopy showed that the BSMs were regular, uniform in size and without aggregation. Small holes were noted on the surface of microspheres (Figure 1). BSMs dispersed well in normal saline and omnipaque. The concentration of microspheres in solution had no effect on the suspension time. The size of microspheres had a significant effect on the suspension time. The settling time was approximately 4–6 min in omnipaque, and approximately 2–3 min in normal saline. In general, the settling times in these 2

situations were long enough for syringe drawing. The microspheres went well through 5F catheter in both normal saline and omnipaque solution. There was no aggregation and deformation. Microspheres sized less than 400  $\mu\text{m}$  could pass through 3F SP micro-catheter and did not deform and aggregate. For microspheres with diameter larger than 400  $\mu\text{m}$ , it was difficult for them to pass through a 3F SP micro-catheter. They would aggregate, swell and occlude the microcatheter.

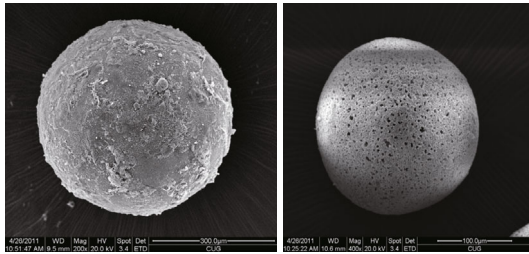


**Figure 1. Photography of Particle by Electron Microscope Scan**

Notes: magnification: left:  $\times 200$ , right:  $\times 400$

**Renal Artery Embolization**

All animals survived after the interventional operation. Embolization was successfully performed in all of the rabbits. In the embolic process, renal artery blood flow slowed down gradually from the distal to proximal and stagnated. A follow-up angiogram immediately after embolization showed a patent renal artery trunk, without staining of the renal parenchyma. At the other follow-up time point, the angiogram showed that vascular network existed and renal parenchyma was stained in the contralateral untreated kidney. In the BSMs group, there was no evidence of collateral circulation formation in the embolized renal artery in the experimental group at all observation time points (Figure 2). However, in the control group, abundant new blood vessels were formed in the renal capsule, which developed into renal parenchyma after 14 days.

As shown in Figure 3, the tissue surrounding the embolized renal tissue appeared edematous and

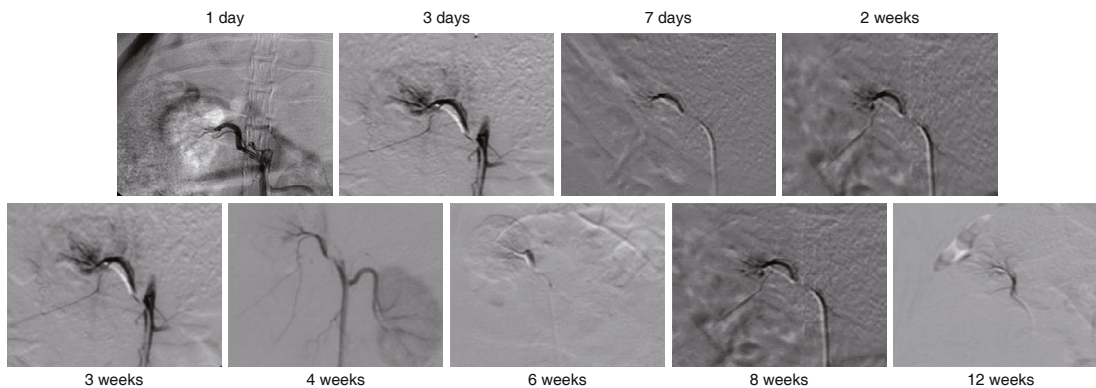


**Figure 2. Angiography Performance after Right Renal Artery Embolization at Different Times with BSMs Intervention in Rabbits**

Note: The right renal artery was embolized completely with no collateral circulation angiogenesis

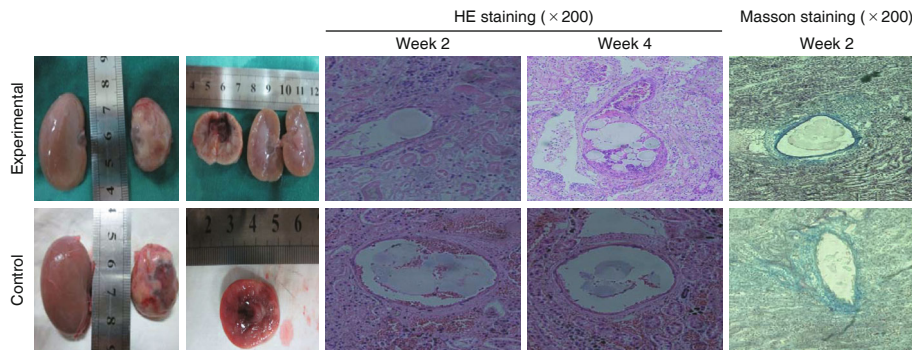


**Figure 3. Pathological Manifestation of Rabbit Kidney**

Notes: In the experimental group, the right kidney surface was yellow, with bleeding points, the volume was reduced compared with the contralateral kidney at 4 weeks, with an ill-defined cortex and medulla, and partial necrosis; BSMs in the renal blood vessels at 2 and 4 weeks, respectively. After 4 weeks, the edge of BSMs showed defects and broke; after 2 weeks, renal artery vascular showed that the vessel wall stained light blue, with vascular wall integrity, no rupture, and no defects. While in the control group, PVA particles were present in the renal artery and the injured vessel wall after 4 weeks. PVAs in the renal blood vessels at 2 and 4 weeks, respectively. The appearance of the PVAs showed irregular

the surface was dark red, piebald-like or showed bleeding in the first day post-embolization. However, 2 weeks later, the surface turned yellow and the boundary between the cortex and medulla was ill-defined. At week 3, the kidney surface was grainy and the contralateral kidney showed compensatory hypertrophy. At week 4, the texture of the embolized kidney was hard, and the necrotic area was visible on the surface. Similar findings were noted on week 6–12; however, the extent of fibrosis was more severe than week 4. The texture was harder and tougher. A small, yellow calcified area was visible on the kidney surface, which on touch, felt similar to sand. The corticomedullary boundary disappeared completely. The degree of arterial inflammation was similar between the two groups. The infiltrating inflammatory cells at week 1 were mainly neutrophils and lymphocytes, and after 1 week, were mainly neutrophils. BSMs remain in the prototype before 4 weeks. After 4 weeks, the microspheres gradually manifested edge defects, such as irregularity, which caused them to break. Vascular elastic membrane was stained as blue ribbon. In the control group, vessel wall injury was not obvious at week 2, gradually increased at week 4, and alleviated after 6 weeks. On the contrary, the vessel wall injury was not obvious in the experimental group. BSMs were not found in the lung tissue.

In both the experimental group and control group, BUN and Cre increased significantly on day 3, peaked on day 7, and returned to normal on day 14 after operation (Figure 4A). ALT and AST increased in the first 3 days after embolization, and returned to normal on day 7 (Figure 4B). At each observation time point, there were no significant differences in AST, ALT, BUN and Cre between groups ( $P>0.05$ ).

### Results of Embolization in Rabbit Liver VX2 Tumor Model

The results of rabbit VX2 tumor treatment in each group are shown in Table 1 and Figure 5. Differences in tumor GR, AI, apoptosis-related factors bax, bcl-2 and VEGF between groups B and C were not significant ( $P>0.05$ ). However, there were significant differences between groups B, C and group A ( $P<0.05$ ).

In the BSMs group, it was noted that there

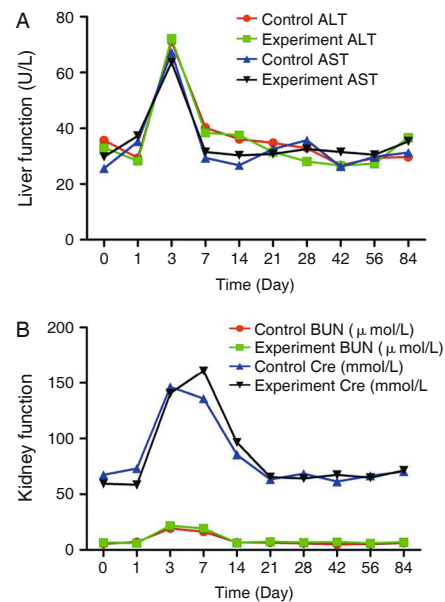


**Figure 4. Liver (A) and Kidney (B) Function Changes after Rabbit Renal Artery Embolization in Different Period**

**Table 1. Comparison of Tumor GR, AI, Apoptosis-Related Factors and VEGF Levels of Liver VX2 Tumor Model in Rabbits among Groups ( $\bar{x} \pm s$ )**

Group	GR (%)	AI	Bax	Bcl-2	VEGF
A	5.9	8.2 ± 1.2	4.1 ± 1.3	21.6 ± 4.5	12.4 ± 3.2
B	2.4**	14.5 ± 2.5**	8.7 ± 2.2**	13.2 ± 2.7**	19.3 ± 5.7*
C	2.7**	16.3 ± 3.7**	7.4 ± 2.5*	14.6 ± 2.8**	17.5 ± 4.2*

Notes: \* $P<0.05$ , \*\* $P<0.01$  vs. group A

was no recanalization of tumor blood vessels and collateral vascular formation on postoperative hepatic angiography. The tumor presented with complete necrosis in gross-view, fibrous non-organized tissue instead of tumor structure in microscopic view, and the BSMs could be observed. Apoptotic cells showed brown-yellow granules in nuclei of cancer cells, which were located at the necrotic area around the tumor with a diffuse or spotty distribution, or at the residual viable tumor area with a scattered distribution. The hot-spot of apoptotic cells was located in the tumor margin, especially in the tumor-infiltrated capsule. The expression of the apoptosis-related genes, bcl-2 and bax, were mainly localized in the cytoplasm of cancer cells and some interstitial tissue, with slight expression in both tumor cell cytoplasm and cell membrane, with a spotty or sheet-like distribution. VEGF was diffusely or focally expressed in some cancer nests, especially in tumor margin and in necrotic zone. Serial sections showed more positive capillaries surrounding the cancer nest, and there was no VEGF expression in

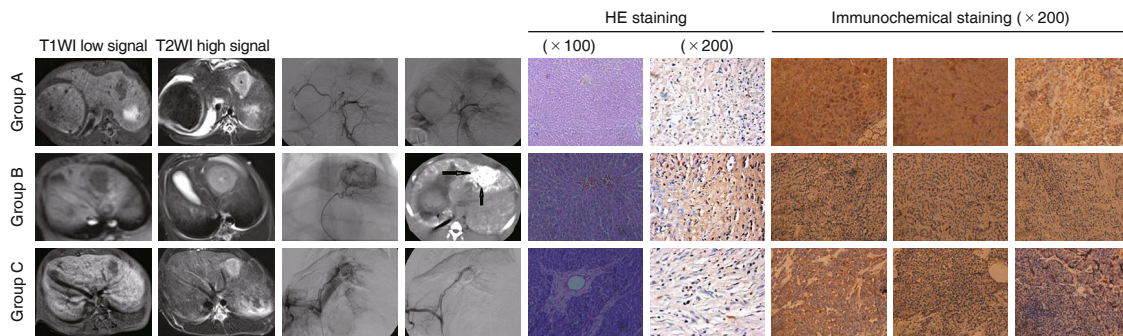


**Figure 5. VX2 Tumor in Left Lobe of Rabbit Liver before and after Embolization by BSMs**

Notes: In group A, the staining was obvious after saline perfusion, there was no embolic agent and little apoptotic body. In group B, the apoptotic body was obvious. In group C, BSMs was seen at the tumor vessel, the apoptotic body was obvious.

normal liver tissue.

## DISCUSSION

In this study, a series of BSMs in different diameter were prepared with the modified method of Emulsion-condensation-chemical cross linking and sized by passing them through sieves with different apertures. Electron microscopy and light microscopy scanning confirmed that the uniform size distribution of microspheres and small holes were formed on the surface of microspheres. It overcame the disadvantage of low yield ratio, a wide particle size distribution and poor reproducibility.<sup>(10-12)</sup> This process yielded different diameters of particles that could be selected as needed, thus avoiding the complications of extrahepatic embolism<sup>(13,14)</sup> due to embolization by small particles, thereby achieving a controllable ideal embolization effect.<sup>(15)</sup> The holes on the surface of microspheres would be able to carry anti-cancer drugs or genes.

Microspheres are usually dispersed in iodine-containing contrast agents for embolization. The dispersion and deposition time of microsphere suspension in contrast agent influences the withdrawing into and injection from the syringe. Microspheres expand when setting in contrast agent. If the swelling is too fast, the microsphere will be broken easily and contributed to the interventional operation difficultly. It is a requisite that the microspheres should not be deformed or show only a slight deformation during the injection through the catheter.<sup>(16)</sup> If the swelling coefficient is too large, the quickly expanded microspheres will embolize blood vessels immediately, and thus cannot move to distal tumor vessels and achieve the desired effect of embolization.<sup>(17)</sup> It is generally believed that if the vessels embolized by a

particular type of microspheres are not recanalized, this type of microsphere is a medium-term embolic agent.<sup>(18)</sup> This experiment demonstrated that BSMs swelled quickly in saline and contrast agent, and reached the maximum swelling after 30 min. However, there was enough time for syringe extraction before embolization. BSMs maintained their intact morphology, even after maximum swelling, and broke *in vitro* after 6 weeks. *In vitro* experiments showed that all sizes of BSMs maintained their integrity of shape when passed through the 5F catheter. However, it was difficult for the BSMs no less than 400 μm in size to pass through a 3F micro-catheter, which was due to the swelling of microspheres.<sup>(19)</sup>

In this study, the BSMs used in renal artery embolization were 200 μm in diameter. They embolized interlobular arteries,<sup>(20)</sup> and no collateral circulation formation on angiography in the experimental group until 12 weeks after embolization. However, collateral circulation formation occurred in the control group. This indicated that BSMs embolized more thoroughly than PVA. It is well known that PVA is a long-term embolic agent.<sup>(21)</sup> This study indicated that BSM is a mid-term embolic agent. Similar changes of liver and kidney functions and perivascular inflammatory cell response were noted in both experimental group and control group. This demonstrates that the BSMs had the same biocompatibility as PVA. Trans-arterial chemoembolization is the preferred method of treatment for unresectable liver carcinoma.<sup>(22)</sup> Conventionally, as a drug carrier, lipiodol has a good mobility, and can selectively stay in the tumor tissue.<sup>(23)</sup> Meanwhile, the emulsion of lipiodol and chemotherapeutic drugs are unstable, releasing drugs very quickly, which can cause side effects.<sup>(24,25)</sup> On the other hand, collateral circulation formation

after embolization will affect the long-term treatment efficacy.<sup>(26)</sup> BSMs could be prepared as needed and injected into the hepatic artery prior to the sinusoidal level of small arteries.<sup>(27)</sup> Compared with other embolic agents, it embolizes the tumor vasculatures more thoroughly and does not form collateral circulation.

The bcl-2 gene family plays an important role in the regulation of apoptosis. Specifically, a number of bcl-2 gene families can inhibit apoptosis, but the expression of bax can inhibit bcl-2 function to promote apoptosis.<sup>(28)</sup> VEGF is one of the strongest, well-known angiogenic growth factors<sup>(29)</sup> that can create the conditions that promote tumor invasion and metastasis. In this study, BSMs not only inhibited the tumor growth and promoted tumor cell apoptosis, but also inhibited the tumor vascular collateral circulation, which could lead to recurrence and metastasis. The experimental group had the lower expressions of VEGF due to the apoptosis mechanism, and angiogenesis is an essential step in tumor growth.<sup>(30)</sup> Therefore, the BSMs is very promising in suppressing tumor growth by inducing apoptotic cell death and through anti-proliferative on cancer cells of VEGF. The VEGF is secreted by tumor cells and stimulates the growth of endothelial cells, usually in response to external stimuli such as hypoxia or substances secreted by the body.<sup>(31)</sup> As such, BSMs have microsphere embolism features.<sup>(32,33)</sup>

It should be noted that in our study BSMs have a preliminary character, because after more than ten years of efforts and improvement, it has not produced to the market. The re-standardization of the production of BSMs was to prepare for the market. The shortcomings of this study were that with repeatedly place compared with the previous research and the research has not been carried out in the production of drug-loading research of BSMs. The next step would be carried out the research of BSMs loading hepatic tumor suppressor gene.

In summary, BSMs prepared by this modified method is in full compliance with the requirement for use in interventional procedures and is an ideal midterm embolic agent.

### Conflict of Interest

The authors declare that they have no competing interests.

### Author Contributions

Luo SH designed the research, carried out the experiments and wrote the manuscript text. Song SL prepared the figures and tables. Li WY responsible for microsphere preparation. Xia XW developed methodology. Wang Y performed data analysis. Zheng CS and Feng GS was responsible for experimental design and supervised the study.

### REFERENCES

1. Bilbao JI, de Martino A, de Luis E, Díaz-Dorransoro L, Alonso-Burgos A, Martínez de la Cuesta A, et al. Biocompatibility, inflammatory response, and recanalization characteristics of nonradioactive resin microspheres: histological findings. *Cardiovasc Intervent Radiol* 2009;32:727-736.
2. Derdeyn CP, Graves VB, Salamat MS, Rappe A. Collagen-coated acrylic microspheres for embolotherapy: *in vivo* and *in vitro* characteristics. *AJNR Am J Neuroradiol* 1997;18:647-653.
3. Yamamoto A, Imai S, Kobatake M, Yamashita T, Tamada T, Umetani K. Evaluation of tris-acryl gelatin microsphere embolization with monochromatic X rays: comparison with polyvinyl alcohol particles. *J Vasc Interv Radiol* 2006;17:1797-1802.
4. Qian J, Vossoughi D, Woitaschek D, Oppermann E, Bechstein WO, Li WY, et al. Combined transarterial chemoembolization and arterial administration of *Bletilla striata* in treatment of liver tumor in rats. *World J Gastroenterol* 2003;9:2676-2680.
5. Feng G, Kramann B, Zheng C, Zhou R. Comparative study on the long-term effect of permanent embolization of hepatic artery with *Bletilla striata* in patients with primary liver cancer. *J Tongji Med Univ* 1996;16:111-116.
6. Zheng C, Feng G, Liang H. *Bletilla striata* as a vascular embolizing agent in interventional treatment of primary hepatic carcinoma. *Chin Med J* 1998;111:1060-1063.
7. Dong L, Xia S, Luo Y, Diao H, Zhang J, Chen J, et al. Targeting delivery oligonucleotide into macrophages by cationic polysaccharide from *Bletilla striata* successfully inhibited the expression of TNF-alpha. *J Control Release* 2009;134:214-220.
8. Wu XG, Xin M, Chen H, Yang LN, Jiang HR. Novel mucoadhesive polysaccharide isolated from *Bletilla striata* improves the intraocular penetration and efficacy of levofloxacin in the topical treatment of experimental bacterial keratitis. *J Pharm Pharmacol* 2010;62:1152-1157.
9. Luo Y, Diao H, Xia S, Dong L, Chen J, Zhang J. A physiologically active polysaccharide hydrogel promotes wound healing. *J Biomed Mater Res A* 2010;94:193-204.
10. Nakashima T, Shimizu M, Kukizaki M. Particle control of emulsion by membrane emulsification and its applications.

- Adv Drug Deliv Rev 2000;45:47-56.
11. Dalpiaz A, Scatturin A, Pavan B, Biondi C, Vandelli MA, Forni F. Poly (lactic acid) microspheres for the sustained release of antiischemic agents. *Int J Pharm* 2002;242:115-120.
  12. Tran VT, Benoît JP, Venier-Julienne MC. Why and how to prepare biodegradable, monodispersed, polymeric microparticles in the field of pharmacy? *Int J Pharm* 2011;407:1-11.
  13. Nozari A, Dilekoz E, Sukhotinsky I, Stein T, Eikermann-Haerter K, Liu C, et al. Microemboli may link spreading depression, migraine aura, and patent foramen ovale. *Ann Neurol* 2010;67:221-229.
  14. Cook DJ, Zehr KJ, Orszulak TA. Reduction in brain embolization using the *Aegis aortic* cannula during bypass in swine. *Ann Thorac Surg* 2002;74:825-829.
  15. Ma KF, Wong WH, Lui CY, Cheng LF. Renal and splenic micro-infarctions following bronchial artery embolization with tris-acryl microspheres. *Kor J Radiol* 2009;10:97-99.
  16. Kang MJ, Park JM, Choi WS, Lee J, Kwak BK, Lee J. Highly spherical and deformable chitosan microspheres for arterial embolization. *Chem Pharm Bull* 2010;58:288-292.
  17. Siewiorek GM, Wholey MH, Finol EA. *In vitro* performance assessment of distal protection filters: pulsatile flow conditions. *J Endovasc Ther* 2009;16:735-743.
  18. Ohta S, Nitta N, Takahashi M, Murata K, Tabata Y. Degradable gelatin microspheres as an embolic agent: an experimental study in a rabbit renal model. *Kor J Radiol* 2007;8:418-428.
  19. van Hooy-Corstjens CS, Saralidze K, Knetsch ML, Emans PJ, de Haan MW, Magusin PC, et al. New intrinsically radiopaque hydrophilic microspheres for embolization: synthesis and characterization. *Biomacromolecules* 2008;9:84-90.
  20. Ohta S, Nitta N, Sonoda A, Seko A, Seko A, Tanaka T, Takazakura R, et al. Embolization materials made of gelatin: comparison between Gelpart and gelatin microspheres. *Cardiovasc Intervent Radiol* 2010;33:120-126.
  21. Lee KH, Liapi E, Ventura VP, Buijs M, Vossen JA, Vali M, et al. Evaluation of different calibrated spherical polyvinyl alcohol microspheres in transcatheter arterial chemoembolization: VX2 tumor model in rabbit liver. *J Vasc Interv Radiol* 2008;19:1065-1069.
  22. Raoul JL, Sangro B, Forner A, Mazzaferro V, Piscaglia F, Bolondi L, et al. Evolving strategies for the management of intermediate-stage hepatocellular carcinoma: available evidence and expert opinion on the use of transarterial chemoembolization. *Cancer Treat Rev* 2011;37:212-220.
  23. Takayasu K, Arii S, Ikai I, Kudo M, Matsuyama Y, Kojiro M, et al. Overall survival after transarterial lipiodol infusion chemotherapy with or without embolization for unresectable hepatocellular carcinoma: propensity score analysis. *Am J Roentgenol* 2010;194:830-837.
  24. Liapi E, Geschwind JF. Intra-arterial therapies for hepatocellular carcinoma: where do we stand? *Ann Surg Oncol* 2010;17:1234-1246.
  25. Marelli L, Shusang V, Buscombe JR, Cholongitas E, Stigliano R, Davies N, et al. Transarterial injection of <sup>131</sup>I-lipiodol, compared with chemoembolization, in the treatment of unresectable hepatocellular cancer. *J Nucl Med* 2009;50:871-877.
  26. Sueyoshi E, Hayashida T, Sakamoto I, Uetani M. Vascular complications of hepatic artery after transcatheter arterial chemoembolization in patients with hepatocellular carcinoma. *Am J Roentgenol* 2010;195:245-251.
  27. Ibrahim SM, Lewandowski RJ, Sato KT, Gates VL, Kulik L, Mulcahy MF, et al. Radioembolization for the treatment of unresectable hepatocellular carcinoma: a clinical review. *World J Gastroenterol* 2008;14:1664-1669.
  28. Antonsson B. Mitochondria and the Bcl-2 family proteins in apoptosis signaling pathways. *Mol Cell Biochem* 2004;256-257:141-155.
  29. Roukos DH, Tzacos A, Zografos G. Current concerns and challenges regarding tailored anti-angiogenic therapy in cancer. *Expert Rev Anticancer Ther* 2009;9:1413-1416.
  30. Szegezdi E, Macdonald DC, NiChonghaile T, Gupta S, Samali A. Bcl-2 family on guard at the ER. *Am J Physiol Cell Physiol* 2009;296:C941-C953.
  31. Makrilia N, Lappa T, Xyla V, Nikolaidis I, Syrigos K. The role of angiogenesis in solid tumours: an overview. *Eur J Intern Med* 2009; 20:663-671.
  32. Verret V, Ghegediban SH, Wassef M, Pelage JP, Golzarian J, Laurent A. The arterial distribution of Embosphere and Embosphere microspheres in sheep kidney and uterus embolization models. *J Vasc Interv Radiol* 2011;22:220-228.
  33. Shomura Y, Tanigawa N, Shibutani M, Wakimoto S, Tsuji K, Tokuda T, et al. Water-soluble polyvinyl alcohol microspheres for temporary embolization: development and in vivo characteristics in a pig kidney model. *J Vasc Interv Radiol* 2011;22:212-219.

(Accepted July 26, 2016; First Online May 11, 2017)

Edited by YUAN Lin